Thermodynamics and quantum corrections from molecular dynamics for liquid water

Peter H. Berens, Donald H. J. Mackay, Gary M. White, and Kent R. Wilson

Citation: J. Chem. Phys. **79**, 2375 (1983); doi: 10.1063/1.446044
View online: http://dx.doi.org/10.1063/1.446044
View Table of Contents: http://jcp.aip.org/resource/1/JCPSA6/v79/i5
Published by the American Institute of Physics.

Thermodynamics and quantum corrections from molecular dynamics for liquid water

Peter H. Berens, Donald H. J. Mackay, Gary M. White, and Kent R. Wilson

Department of Chemistry, University of California-San Diego, La Jolla, California 92093
(Received 18 October 1982; accepted 19 May 1983)

In principle, given the potential energy function, the values of thermodynamic variables can be computed from statistical mechanics for a system of molecules. In practice for the liquid state, however, two barriers must be overcome. This paper treats the first problem, how to quantum correct the classical mechanical thermodynamic values available from molecular dynamics, Monte Carlo, perturbation, or integral methods in order to compare with experimental quantum reality. A subsequent paper will focus on the second difficulty, the effective computation of free energy and entropy. A simple technique, derived from spectral analysis of the atomic velocity time histories, is presented here for the frequency domain quantum correction of classical thermodynamic values. This technique is based on the approximation that potential anharmonicities mainly affect the lower frequencies in the velocity spectrum where the system behaves essentially classically, while the higher spectral frequencies, where the deviation from classical mechanics is most pronounced, involve sufficiently harmonic atomic motions that harmonic quantum corrections apply. Thus, a harmonic quantum correction can be applied at all frequencies: at low frequencies where it is inaccurate it will be small, while at high frequencies where it is large it will also be relatively accurate. The approach is demonstrated by computation of the energy and constant volume heat capacity for water from classical molecular dynamics followed by quantum correction. The potential used to describe the interactions of the system of water molecules includes internal vibrational degrees of freedom and thus strong quantum effects. Comparison of the quantum corrected theoretical values with experimental measurements shows good agreement. The quantum corrections to classical thermodynamics (which are also derived for free energy and entropy) are shown to be important not only for internal vibrational motion, but also for intermolecular hindered rotational and translational motions in liquid water. They are presumably also important for other strongly associated molecules, including bimolecules, and thus should be included when comparing calculated and measured thermodynamic quantities. The approach illustrated here allows the calculation of thermodynamic quantum corrections for liquids, solutions, and large molecules such as polymers (including proteins and nucleic acids) with full inclusion of both intra- and intermolecular degrees of freedom.

I. INTRODUCTION

In principle from the potential energy as a function of nuclear positions one can compute from statistical mechanics the values of the thermodynamic variables. In practice this has been a difficult task for liquids and larger molecules such as proteins and nucleic acids. Two substantial barriers need to be overcome. The first, which is the subject of this paper, is how to compute *quantum* thermodynamic reality when only *classical* mechanics is practically available as a computational tool. That quantum mechanics is essential in treating intramolecular vibrations is universally acknowledged, but it has sometimes been less well appreciated that intermolecular motions in strongly associated liquids like water also show important quantum effects. Quantum corrections should thus be considered for strongly interacting molecules in general, even for molecules approximated as rigid bodies, and for biomolecules. The second barrier which is the subject of a paper to follow, is how to practically compute the useful, but intrinsically difficult, free energy and entropy.

The present paper illustrates a simple molecular dynamics technique for quantum correcting classical thermodynamic quantities, e.g., those derived from molecular dynamics, Monte Carlo, perturbation, or integral methods. This approach makes use of the velocity spectrum (often called the velocity autocorrelation spectrum). For harmonic systems the spectrum is directly linked to both classical and quantum mechanical thermodynamic parameters, as it then represents the density of normal mode harmonic oscillators as a function of frequency. Two suppositions are used to justify a harmonic approach to estimating the thermodynamic quantum corrections: (i) that anharmonicities mainly affect the low frequency motions which are nearly classical, and (ii) that high frequency motions, where quantum effects are more important, are nearly harmonic. With these assumptions the quantum corrections for a thermodynamic variable can be evaluated simply from the integral over frequency of a universal weighting function for that variable times the velocity spectrum computed from power spectra of atomic velocity time histories. The weighting functions approach zero in the low frequency region where anharmonicities would otherwise cause problems. Such a quantum correction approach is not limited, like most other approaches, to nearly classical systems, but can equally be used to treat molecular systems with internal vibrational degrees of freedom where quantum effects are very strong, e.g., molecular liquids, solutions, solids, and polymers, including proteins and nucleic acids, with full inclusion of internal degrees of freedom.

Section II describes the classical calculation of energy, heat capacity, free energy, and entropy from molecular dynamics, followed in Sec. III with the theory of our quantum correction technique. Section IV de-

 0021-9606/83/172375-15$02.10

scribes the calculation and quantum correction of the energy and heat capacity of liquid water. While quite good agreement is achieved with experiment, we emphasize that our main purpose is to illustrate the techniques and not to make the most accurate possible thermodynamic calculations. We point out that the choice of boundary treatment can significantly affect the numerical results. Section V discusses these results and their meaning.

II. CLASSICAL THERMODYNAMICS FROM MOLECULAR DYNAMICS

The standard equations[1] linking the canonical partition function Q and the various thermodynamic variables are

$$E = k_B T^2 \frac{\partial \ln Q}{\partial T} , \tag{2.1}$$

$$C_v = \frac{\partial E}{\partial T} , \tag{2.2}$$

$$A = -k_B T \ln Q , \tag{2.3}$$

$$S = k_B T \frac{\partial \ln Q}{\partial T} + k_B \ln Q , \tag{2.4}$$

in which E is the energy, C_v the constant volume heat capacity, A the Helmholtz free energy, S the entropy, k_B Boltzmann's constant, and T the temperature.

A. Energy

The energy at a given temperature T may be computed from molecular dynamics in several ways. (i) Choose initial conditions for a set of different constant energy microcanonical molecular dynamics runs to approximate a canonical ensemble at T, e.g., by a sequence of kinetic energy randomizations from a Boltzmann distribution. The classical energy of the system

$$E = \langle E_k(\mathbf{p}^N) + V(\mathbf{r}^N) \rangle \tag{2.5}$$

is then derived as an average, symbolized by $\langle\ \rangle$, over several molecular dynamics runs from the ensemble at temperature T in which E_k is the kinetic energy and V the potential energy, letting the positions and momenta of the N atoms be represented by $\mathbf{r}^N \equiv \mathbf{r}_1, \ldots, \mathbf{r}_N$ and $\mathbf{p}^N \equiv \mathbf{p}_1, \ldots, \mathbf{p}_N$, respectively. (ii) Compute the temperature for several different runs at different constant values of the total energy by averaging the instantaneous temperature defined in terms of the kinetic energy by

$$\langle T(t) \rangle = (3Nk_B)^{-1} \sum_{j=1}^{3N} m_j \langle (\mathbf{v}_j(t))^2 \rangle , \tag{2.6}$$

where $\mathbf{v}_j$ is a Cartesian component of the velocity of one of the N atoms, m_j is the mass of that atom, and $\langle\ \rangle$ here indicates a time average. Fit an energy vs temperature curve to the results for several such microcanonical molecular dynamics runs. (iii) Adjust the kinetic energies during each molecular dynamics run in order to represent the system in a heat bath at temperature T as demonstrated by Andersen.[2] In this paper we use both approaches (i) and (ii).

B. Heat capacity

By performing microcanonical molecular dynamics runs at several different energies and computing the average temperature for each energy, in other words method (ii) above, the heat capacity at constant volume C_v can be derived through numerical differentiation of energy E with respect to the temperature T.

In addition, the heat capacity may be calculated in principle from the kinetic energy fluctuation for a microcanonical ensemble. With the velocity of the center of mass set to zero, the heat capacity is given by[3,4]

$$C_v = R \Big/ \left[\frac{2}{3} - N \left(\frac{\langle T^2 \rangle - \langle T \rangle^2}{\langle T \rangle^2} \right) \right] \tag{2.7}$$

in which R is k_B times Avogadro's number, the number of atoms is N, and T is defined as in Eq. (2.6) above. Statistical accuracy becomes very important as the denominator becomes small, which possibly explains why we did not succeed in calculating accurate values using this approach.

C. Free energy and entropy

The free energy may be computed from molecular dynamics by a technique due to Kirkwood[1,5] which has been applied in a parallel manner to Monte Carlo calculations,[6] as demonstrated by Mezei, Swaminathan, and Beveridge[7] in a classical Monte Carlo calculation of the free energy of rigid molecule liquid water.

The classical canonical ensemble partition function $Q(\xi)$ is defined as[1]

$$Q(\xi) = (N!h^{3N})^{-1} \iint d\mathbf{r}^N d\mathbf{p}^N \exp[-\beta H(\mathbf{r}^N, \mathbf{p}^N, \xi)] \tag{2.8}$$

in which $H(\mathbf{r}^N, \mathbf{p}^N, \xi)$ is the classical Hamiltonian of the system, the Kirkwood[1,5-7] ξ is a parameter upon which the Hamiltonian depends, and $\beta \equiv (k_B T)^{-1}$. Equation (2.3) now gives

$$A(\xi) = -\beta^{-1} \ln Q(\xi). \tag{2.9}$$

Differentiating Eq. (2.9) with respect to ξ gives

$$\frac{\partial A(\xi)}{\partial \xi} = -\beta^{-1} \frac{\partial \ln Q(\xi)}{\partial \xi} , \tag{2.10}$$

which allows us to write

$$A(\xi_2) - A(\xi_1) = -\beta^{-1} \int_{\xi_1}^{\xi_2} d\xi \frac{\partial \ln Q(\xi)}{\partial \xi} , \tag{2.11}$$

in which ξ_2 is the value of the Kirkwood parameter which gives the real Hamiltonian and ξ_1 is a value which distorts the Hamiltonian to give a reference system (e.g., an ideal gas, a hard sphere liquid, or a harmonic solid) for which we can more easily compute the free energy.[8] Using Eq. (2.8), we have

$$\frac{\partial \ln Q(\xi)}{\partial \xi} = \frac{1}{Q(\xi)} \frac{\partial Q(\xi)}{\partial \xi}$$

$$= \frac{-\beta (N!h^{3N})^{-1} \iint d\mathbf{r}^N d\mathbf{p}^N \frac{\partial H(\mathbf{r}^N, \mathbf{p}^N, \xi)}{\partial \xi} \exp[-\beta H(\mathbf{r}^N, \mathbf{p}^N, \xi)]}{Q(\xi)} \tag{2.12}$$

which by the ensemble postulate of Gibbs

$$= -\beta \left\langle \frac{\partial H(\mathbf{r}^N, \mathbf{p}^N, \xi)}{\partial \xi} \right\rangle_\xi , \tag{2.13}$$

where the derivative of the Hamiltonian with respect to ξ is averaged over coordinates and momenta from an ensemble with the Hamiltonian containing the parameter ξ. Substituting Eq. (2.13) into Eq. (2.11) gives

$$A(\xi_2) - A(\xi_1) = \int_{\xi_1}^{\xi_2} d\xi \left\langle \frac{\partial H(\mathbf{r}^N, \mathbf{p}^N, \xi)}{\partial \xi} \right\rangle_\xi . \quad (2.14)$$

To evaluate Eq. (2.14) by molecular dynamics, atomic trajectories are computed for the Hamiltonian $H(\mathbf{r}^N, \mathbf{p}^N, \xi)$, $[\partial H(\mathbf{r}^N, \mathbf{p}^N, \xi)]/(\partial \xi)$ is averaged over an ensemble of these trajectories at temperature T, and the result is then integrated between ξ_1 and ξ_2.

In this way, the classical free energy change between the system with our real Hamiltonian $H(\mathbf{r}^N, \mathbf{p}^N, \xi_2)$ and a reference system with Hamiltonian $H(\mathbf{r}^N, \mathbf{p}^N, \xi_1)$ can be computed. We choose the reference system to be one for which we can compute the classical free energy more tractably.

The entropy S of the system may then be calculated using

$$S = (E - A)/T . \quad (2.15)$$

We will illustrate in a subsequent paper the actual molecular dynamics calculation and quantum correction of the free energy and entropy of liquid water using approaches based on the Kirkwood technique.

III. QUANTUM CORRECTIONS FROM CLASSICAL MOLECULAR DYNAMICS

Outside of the trivial correction for vibrational zero point energy which may be calculated from spectroscopic data[9] and which is generally introduced as a constant in the potential function, the vast majority of work in quantum corrections to classical thermodynamic computations stems from a method first introduced by Wigner[10] and Kirkwood.[11,12] In this approach the free energy is expanded in powers of h^2, and the first term in the quantum correction to be added to the classical value of the free energy is shown to be proportional to the classically averaged sum of the squares of the forces exerted on the particles in the system. The Wigner–Kirkwood technique has been modified, extended and tested by many workers.[13–21] Others[22–31] have examined various methods to handle nondifferentiable potential functions which apply, e.g., to hard spheres or square wells. Barker and Henderson have written a comprehensive review of liquids which includes an extensive section on quantum corrections.[6]

Another quantum correction method by Doll and Myers[32] is based on the path integral approach of Feynman and Hibbs.[33] It involves the calculation of an effective potential V_{eff} in the first stage of a Monte Carlo technique. In the second state, V_{eff} is used to calculate the ratio between the quantum mechanical and classical partition functions. Stillinger[34] discusses the easier calculation of effective potentials for pairwise potentials.

In addition to the quantum corrections considered here there are the effects of the symmetry restrictions on quantum states imposed by Fermi–Dirac and Bose–Einstein statistics. In the temperature range of interest here these effects are negligible.[11,12,35]

A disadvantage of all the previously cited techniques, except the vibrational zero point energy correction, is that they are ordinarily restricted to systems with small quantum effects. The method we present in this paper may be applied when quantum corrections are large, e.g., to intramolecular vibrations.

Owicki and Scheraga[36] discuss the quantum corrections for liquid water. Using approximations to the effects of librational and vibrational frequencies, they calculate the quantum mechanical contributions from vibrational motion to energy and constant pressure heat capacity. These quantum contributions minus the classical values give their quantum corrections. They discuss the shift in the vibrational frequency of water as it enters the liquid phase which changes the zero point energy. This is necessary because they use rigid molecules. The type of nonrigid potential which we use includes both intra- and intermolecular degrees of freedom and thus in principle (but not yet in practice due to potential energy function inaccuracies as is discussed below) can take into account the frequency changes from gas to liquid.

The quantum correction technique used in the present paper involves calculating the velocity spectrum $S(\nu)$ from molecular dynamics and then integrating $S(\nu)$ over all frequencies with a weighting function which is the difference between the quantum and classical harmonic weighting functions for the thermodynamic variable of interest.

A. Velocity spectrum

The velocity spectrum $S(\nu)$ of a classical system of N atoms in equilibrium is defined as

$$S(\nu) = 4\pi\beta \sum_{j=1}^{3N} m_j \langle D[\mathbf{v}_j(t)] \rangle , \quad (3.1)$$

in which m_j is the mass of the atom corresponding to the jth Cartesian velocity component as a function of time $\mathbf{v}_j(t)$, and $\langle\ \rangle$ indicates an average over the ensemble. The spectral density operator D (for which windowing and window correction techniques are described elsewhere[37,38]) is evaluated in terms of probability per unit angular frequency,

$$D[\mathbf{v}_j(t)] \equiv (2\pi)^{-1} \lim_{\tau\to\infty} \frac{1}{2\tau} \left| \int_{-\tau}^{\tau} dt \exp(-i2\pi\nu t)\, \mathbf{v}_j(t) \right|^2 . \quad (3.2)$$

The velocity spectrum may also be computed from the Fourier transform of the velocity autocorrelation function. Note that the velocity spectrum can be computed separately for different subsets of atoms (e.g., different elements, different chemical environments of the same element, or different molecules) and the velocity spectrum $S(\nu)$ can then be computed as a sum of the effects from these different subsets of atoms. Thus, as we will see, the quantum corrections also can be partitioned among the different subsets of atoms. Even though once the dynamics, i.e., the set of velocities $\{v_j(t)\}$, is determined, the quantum corrections may be computed separately for different subsets of atoms, it

should be remembered that normally all atoms together contribute to determining the dynamics.

It will be useful below to know the value of the integral $\int_0^\infty d\nu\, S(\nu)$. The Fourier transform of a real function, e.g., $\mathbf{v}_j(t)$, has an even real part and an odd imaginary part.[39] The square of the absolute value of such a Fourier transform, e.g., $D[\mathbf{v}_j(t)]$, is a real even function. A linear combination of real even functions, e.g., $S(\nu)$, is also a real even function. Therefore $S(-\nu) = S(\nu)$ which allows us to write

$$\int_0^\infty d\nu\, S(\nu) = \int_{-\infty}^\infty d\nu\, S(\nu)/2 \ . \tag{3.3}$$

Substituting Eq. (3.2) into Eq. (3.1) and inserting the result into the right-hand side of Eq. (3.3) gives

$$\int_0^\infty d\nu\, S(\nu) = \beta \int_{-\infty}^\infty d\nu \sum_{j=1}^{3N} m_j \times \left\langle \lim_{\tau\to\infty} \frac{1}{2\tau} \left| \int_{-\tau}^{\tau} dt \exp(-i2\pi\nu t)\mathbf{v}_j(t) \right|^2 \right\rangle . \tag{3.4}$$

Let

$$v_j^\tau(t) = \begin{cases} v_j(t) & \text{if } -\tau < t < \tau \\ 0 & \text{otherwise} , \end{cases} \tag{3.5}$$

and let the Fourier transform of $v_j^\tau(t)$ be $F_j^\tau(\nu)$, i.e.,

$$F_j^\tau(\nu) = \int_{-\infty}^\infty dt \exp(-i2\pi\nu t) v_j^\tau(t) = \int_{-\tau}^{\tau} dt \exp(-i2\pi\nu t)\, \nu_j(t) \ . \tag{3.6}$$

Substituting Eq. (3.6) into Eq. (3.4), exchanging integration and the $\tau\to\infty$ limit, and finally using Parseval's theorem[39] gives

$$\int_0^\infty d\nu\, S(\nu) = \beta \sum_{j=1}^{3N} m_j \left\langle \lim_{\tau\to\infty} \frac{1}{2\tau} \int_{-\tau}^{\tau} d\nu \left| F_j^\tau(\nu) \right|^2 \right\rangle \tag{3.7}$$

$$= \beta \sum_{j=1}^{3N} m_j \left\langle \lim_{\tau\to\infty} \frac{1}{2\tau} \int_{-\tau}^{\tau} dt \left| v_j^\tau(t) \right|^2 \right\rangle \tag{3.8}$$

$$= 2\beta \sum_{j=1}^{3N} \left\langle \lim_{\tau\to\infty} \frac{1}{2\tau} \int_{-\tau}^{\tau} dt\, \frac{m_j}{2} (v_j(t))^2 \right\rangle$$

$$= 2\beta [3N/2\beta] = 3N \ . \tag{3.9}$$

The final substitution is a result of the classical equipartition of energy.[1] Thus, the integral of the velocity spectrum from zero to infinite frequency is just three times the number of atoms, which will be true for any potential, harmonic or not.

The diffusion coefficient has a particularly simple expression in terms of the velocity spectrum. The diffusion coefficient $\bar{D}$ of a particle with position history $\mathbf{r}(t)$ is defined as[40]

$$\bar{D} = \frac{1}{3} \lim_{\tau\to\infty} \frac{1}{2\tau} \langle [\mathbf{r}(\tau) - \mathbf{r}(0)]^2 \rangle \ , \tag{3.10}$$

where $\langle\ \rangle$ indicates an ensemble average or for isotropic systems

$$\bar{D} = \frac{1}{2} \lim_{\tau\to\infty} \frac{1}{2\tau} \langle [x(\tau) - x(-\tau)]^2 \rangle \ , \tag{3.11}$$

where $x(\tau)$ now represents any one of the three Cartesian components of $\mathbf{r}(\tau)$ and the range is changed from $(0,\tau)$ to $(-\tau,\tau)$. If we let $D_0[\nu_j(t)]$ denote the value of the spectral density at zero frequency, then Eq. (3.2) becomes

$$D_0[\mathbf{v}_j(t)] = (2\pi)^{-1} \lim_{\tau\to\infty} \frac{1}{2\tau} [x(\tau) - x(-\tau)]^2 \ . \tag{3.12}$$

Combining Eqs. (3.11) and (3.12) we get

$$\bar{D} = \pi \langle D_0[v_j(t)] \rangle \ . \tag{3.13}$$

If $S(\nu)$ is restricted to equivalent particles, then Eq. (3.1) becomes

$$S(\nu) = 4\pi\beta m \sum_{j=1}^{3M} \langle D[\mathbf{v}_j(t)] \rangle = 12\pi M m \beta \langle D[\mathbf{v}_j(t)] \rangle \ , \tag{3.14}$$

where M particles are being considered each of mass m. Then

$$\langle D_0[\mathbf{v}_j(t)] \rangle = S(0)/12\pi M m \beta \tag{3.15}$$

and thus the diffusion constant $\bar{D}$ is related to the zero frequency value of the velocity spectrum $S(0)$ by

$$\bar{D} = S(0)/12 M m \beta \ , \tag{3.16}$$

in which M is the number of equivalent particles and m is their mass. The most usual application of Eq. (3.16) is to consider the particles to be molecules and to compute the diffusion constant from the zero frequency value of the velocity spectrum of the center-of-mass of the molecules.

B. Harmonic approximation

We quantum correct the classical thermodynamic variables using a harmonic oscillator approximation. This correction is based on a division of the dynamics in frequency space. The low frequency region is viewed as nearly classical but containing the major anharmonic effects, and the high frequency region is viewed as nearly harmonic and thus can be quantum corrected exactly within the limits of the harmonic approximation. Thus we can harmonically quantum correct over the whole frequency range, and get nearly the correct answer because (i) in the low frequency range even though the correction is inaccurate it is small, and (ii) in the high frequency range where the correction is large it is also reasonably accurate.

Consider a system of N atoms as linked by harmonic potentials,

$$V(r^N) = V_0 + \frac{1}{2} \sum_{j,k=1}^{3N} \frac{\partial^2 V}{\partial r_j\, \partial r_k} \Delta r_j \Delta r_k \ , \tag{3.17}$$

in which Δr_j and Δr_k are displacements from a potential minimum and V_0 is the potential energy at that minimum. Such a harmonic situation can be approached classically in the limit of small atomic motions about a potential minimum, i.e., at low temperatures, but one should remember that quantum wave functions sample the potential in a region about the minimum even at absolute zero, and thus anharmonicity, both explicit and due to coupling by finite displacements, will always play a role in real systems. Nonetheless, we believe that at higher

frequencies an analysis which uses the finite temperature classical velocity spectrum interpreted as if it were fully harmonic will usually sufficiently well represent the thermodynamic quantum corrections.

In the harmonic limit, a normal mode analysis allows us to view the system as a set of $3N$ harmonic oscillators. The total canonical partition function Q for the system can then be expressed in terms of the partition functions q_j for the individual modes as

$$Q = \prod_{j=1}^{3N} q_j \tag{3.18}$$

or

$$\ln Q = \sum_{j=1}^{3N} \ln q_j \ . \tag{3.19}$$

If the normal frequencies are continuously distributed we may take the integral

$$\ln Q = \int_0^\infty d\nu S(\nu) \ln q(\nu) \ , \tag{3.20}$$

where $S(\nu)$ is the density of normal modes with frequency ν.

To show that the velocity spectrum of a system of particles linked through harmonic potentials represents the density of normal modes, the $3N$ time varying Cartesian position components $x_1, \ldots, x_{3N}$, are first represented in terms of normal coordinates. We have[41]

$$x_k = (m_k)^{-1/2} \sum_{j=1}^{3N} a_{jk} q_j \ , \tag{3.21}$$

$$q_j = A_j \sin(\omega_j t + \vartheta_j) \ , \tag{3.22}$$

where $q_1, \ldots, q_{3N}$ are the normal coordinates, $\omega_1, \ldots, \omega_{3N}$ are the characteristic normal mode angular frequencies in which $2\pi\nu_j = \omega_j$, A_j is the jth normal mode amplitude, ϑ_j is its phase, and a_{jk} are constants scaled such that

$$\sum_{k=1}^{3N} a_{jk}^2 = 1 \ . \tag{3.23}$$

The kinetic and potential energies in terms of the normal coordinates q_j which have units of length times square root of mass and $\dot{q}_j$ which are the time derivatives, are

$$E_k = \frac{1}{2} \sum_{j=1}^{3N} \dot{q}_j^2 \ , \tag{3.24}$$

$$V = \frac{1}{2} \sum_{j=1}^{3N} \omega_j^2 q_j^2 \ . \tag{3.25}$$

Using Eqs. (3.21) and (3.22) to calculate $\dot{x}_k = v_k$ and inserting the result into Eq. (3.1) we get

$$S(\nu) = 4\pi\beta \sum_{k=1}^{3N} m_k \left\langle D\left[(m_k)^{-1/2} \sum_{j=1}^{3N} a_{jk} \omega_j A_j \cos(\omega_j t + \vartheta_j)\right]\right\rangle . \tag{3.26}$$

The power spectral density of a sinusoidal function is[42]

$$D[A_j \cos(\omega_j t + \vartheta_j)] = \frac{A_j^2}{4} [\delta(\omega + \omega_j) + \delta(\omega - \omega_j)] \ . \tag{3.27}$$

Applying this to Eq. (3.26) gives

$$S(\nu) = 4\pi\beta \sum_{j=1}^{3N} (\omega_j^2 A_j^2/4)[\delta(\omega + \omega_j) + \delta(\omega - \omega_j)] \ , \tag{3.28}$$

where Eq. (3.23) has been used.

Applying the theory of equipartition of energy to Eq. (3.24) we get

$$(2\beta)^{-1} = \langle \dot{q}_j^2/2 \rangle \tag{3.29}$$

$$= \omega_j^2 A_j^2/4 \ , \tag{3.30}$$

in which $\langle\ \rangle$ here denotes a time average. Substituting this into Eq. (3.28) gives as our final result

$$S(\nu) = 2\pi \sum_{j=1}^{3N} [\delta(\omega + \omega_j) + \delta(\omega - \omega_j)]$$

$$= \sum_{j=1}^{3N} [\delta(\nu + \nu_j) + \delta(\nu - \nu_j)] \ . \tag{3.31}$$

Thus $S(\nu)$, the velocity spectrum, which is computed from the Cartesian velocity time histories, is indeed the normal mode density for a harmonic system.

C. Classical weighting functions

The classical partition function for a single harmonic oscillator (normalized as usual to the quantum partition function by the inclusion of h^{-1}) is[1]

$$q^C(\nu) = (\beta h\nu)^{-1} = u^{-1} \ , \tag{3.32}$$

where the superscript C indicates that the variable is derived classically, $u \equiv \beta h\nu$ is the reduced energy of the harmonic oscillator $\beta = (k_B T)^{-1}$, h is Planck's constant, and ν is the frequency of the oscillator. Substituting Eq. (3.32) into Eq. (3.20), and inserting this result into Eqs. (2.1) through (2.4) gives

$$E^C = V_0 + k_B T \int_0^\infty d\nu S(\nu) W_E^C(\nu) \ ; \quad W_E^C(\nu) = 1 \ , \tag{3.33}$$

$$C_v^C = k_B \int_0^\infty d\nu S(\nu) W_{C_v}^C(\nu) \ ; \quad W_{C_v}^C(\nu) = 1 \ , \tag{3.34}$$

$$A^C = V_0 + k_B T \int_0^\infty d\nu S(\nu) W_A^C(\nu) \ ; \quad W_A^C(\nu) = \ln u \ , \tag{3.35}$$

$$S^C = k_B \int_0^\infty d\nu S(\nu) W_S^C(\nu) \ ; \quad W_S^C(\nu) = [1 - \ln u] \ . \tag{3.36}$$

These classical weighting functions $W^C(\nu)$ are shown in Fig. 1. To allow the zero of energy to be set arbitrarily, we include V_0, the energy of the system treated classically if all oscillations are stilled. The expressions for energy and heat capacity reduce to the familiar classical results

$$E^C = V_0 + 3Nk_B T \ , \tag{3.37}$$

$$C_v^C = 3Nk_B \ . \tag{3.38}$$

D. Quantum weighting functions

The quantum mechanical partition function for a single harmonic oscillator is[1]

$$q^Q(\nu) = \frac{e^{-u/2}}{1 - e^{-u}} \ , \tag{3.39}$$

where the superscript Q indicates that the variable is

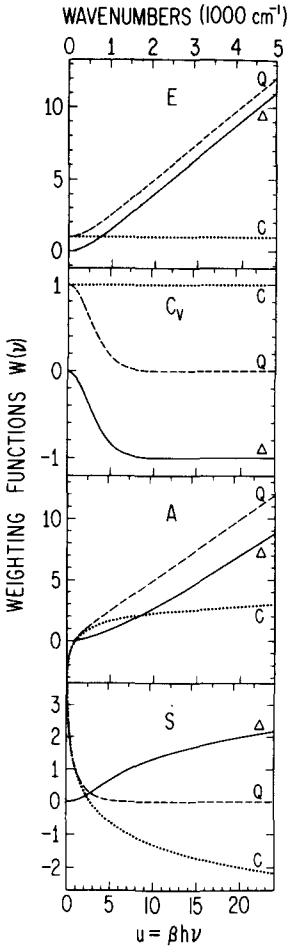

FIG. 1. Universal harmonic weighting functions $W(\nu)$ for the hydrodynamic functions of any harmonic system. Dotted lines are classical $W^C(\nu)$ from Eqs. (3.33) to (3.36), dashed lines are quantum $W^Q(\nu)$, from Eqs. (3.40) to (3.43) and solid lines are quantum correction $W^\Delta(\nu) = W^Q(\nu) - W^C(\nu)$, from Eqs. (3.45)–(3.48). It is thus solid line curves which are used to weight the velocity spectra $S(\nu)$ to compute the quantum corrections to the thermodynamic functions. The top panel is for energy E, the next to the top panel is for constant volume heat capacity C_v, the next to the bottom panel is for Helmholtz free energy A, and the bottom panel is for entropy S. The lower horizontal scale is plotted in reduced energy $u = \beta h\nu$. The upper horizontal scale is the wave number equivalent to u at 300 K. Note that all the quantum correction weighting functions go to zero at low frequency where anharmonic effects become important.

derived quantum mechanically and again $u \equiv \beta h\nu$ is the reduced energy. Substituting Eq. (3.39) into Eq. (3.20) and inserting this result into Eqs. (2.1) through (2.4) gives

$$E^Q = V_0 + k_B T \int_0^\infty d\nu S(\nu)\, W_E^Q(\nu) \; ; \quad W_E^Q(\nu) = \left(\frac{u}{2} + \frac{u}{e^u - 1}\right), \tag{3.40}$$

$$C_v^Q = k_B \int_0^\infty d\nu S(\nu) W_{C_v}^Q(\nu) \; ; \quad W_{C_v}^Q(\nu) = \left(\frac{u^2 e^u}{(1-e^u)^2}\right), \tag{3.41}$$

$$A^Q = V_0 + k_B T \int_0^\infty d\nu S(\nu) W_A^Q(\nu) \; ; \quad W_A^Q(\nu) = \left(\ln \frac{1-e^{-u}}{e^{-u/2}}\right), \tag{3.42}$$

$$S^Q = k_B \int_0^\infty d\nu S(\nu) W_S^Q(\nu) \; ; \quad W_S^Q(\nu) = \left(\frac{u}{e^u - 1} - \ln(1 - e^{-u})\right). \tag{3.43}$$

Fig. 1 shows these quantum weighting functions $W^Q(\nu)$.

For a system which closely approximates a set of harmonic oscillators, such as a perfect crystal at low temperature,[1,8] the above equations alone can be used to compute the thermodynamic variables.

E. Quantum correction weighting functions

The quantum corrections (indicated by the superscript Δ) are obtained by subtracting the classical representations from the quantum mechanical representations for the given thermodynamic variable.

$$W^\Delta(\nu) = W^Q(\nu) - W^C(\nu) \; , \tag{3.44}$$

$$E^\Delta = E^Q - E^C = k_B T \int_0^\infty d\nu S(\nu) W_E^\Delta(\nu) \; ;$$

$$W_E^\Delta(\nu) = \left(\frac{u}{2} + \frac{u}{e^u - 1} - 1\right), \tag{3.45}$$

$$C_v^\Delta = C_v^Q - C_v^C = k_B \int_0^\infty d\nu S(\nu)\, W_{C_v}^\Delta(\nu) \; ;$$

$$W_{C_v}^\Delta(\nu) = \left(\frac{u^2 e^u}{(1-e^u)^2} - 1\right), \tag{3.46}$$

$$A^\Delta = A^Q - A^C = k_B T \int_0^\infty d\nu S(\nu) W_A^\Delta(\nu) \; ;$$

$$W_A^\Delta(\nu) = \left(\ln \frac{1-e^{-u}}{e^{-u/2}} - \ln u\right), \tag{3.47}$$

$$S^\Delta = S^Q - S^C = k_B \int_0^\infty d\nu S(\nu) W_S^\Delta(\nu) \; ;$$

$$W_S^\Delta(\nu) = \left(\frac{u}{e^u - 1} - \ln(1 - e^{-u}) + \ln u - 1\right). \tag{3.48}$$

The quantum correction weighting functions $W^\Delta(\nu)$ are also shown in Fig. 1. Note that following Eqs. (3.1), (3.2), and (3.45)–(3.48) we can partition if we wish the quantum corrections among different subsets of atoms, e.g., different elements, different chemical environments of the same element, different molecules, or molecules in different environments.

IV. MOLECULAR DYNAMICS RESULTS FOR LIQUID WATER

Water is the most important of all solvents, and the molecular level understanding of its bulk properties is of considerable intrinsic interest. We have thus chosen it as a test case for our techniques. A quantum calculation for a system of molecules large enough to adequately represent liquid water is at present impractical, and thus thermodynamic quantities are computed by classical mechanics, usually by Monte Carlo or molecular dynamics techniques. Such classical molecular mechanics calculations on liquid water have been discussed in reviews by Stillinger,[34] Barnes,[43] Wood,[44] and Beveridge *et al.*[45] Goel and Hockney[46] have written a comprehensive bibliography for earlier molecular dynamics in general. It will be shown for liquid water that quantum corrections are needed for both inter- and intramolecular motions to match experimental quantum reality.

A. Liquid water potentials and previous computer simulations

A major obstacle for any molecular mechanics computer simulation is the development of an accurate potential surface. Numerous empirical,[18,47–57] *ab initio*,[58,59] as well as several recent polarizable[60,61] water potentials have been developed. Many molecular dynamic[50,62–75] and Monte Carlo[7,36,45,56–58,71,76–94] calculations have been carried out on liquid water by various authors using most of the potentials cited above. In addition, Weres and Rice[95] discuss the calculation of liquid

water thermodynamic properties and their quantum corrections from a cell model viewpoint. Several papers have tested and compared the variety of water–water potentials, often with disappointing results.[57,96]

The flexible water dimer potential used in this paper is by Watts[97] (WATTS) and consists of a largely empirical intermolecular potential complemented by an intramolecular potential derived from vibrational spectroscopy.[96] The WATTS potential has been studied and criticized by McDonald and Klein.[74,75]

B. Molecular dynamics

Our molecular dynamics calculations are carried out on a system of 250 water molecules at a density of 1.0 g cm^{-3} and a temperature of 300 K with cubic periodic boundary conditions using a special molecular mechanics package running on an array processor.[99,100] Experimentally, this density corresponds to a pressure of 85 atm with a negligible resulting difference[101] of 0.012 kJ mol^{-1} in total energy compared to a pressure of 1 atm which corresponds to a density of 0.997 g cm^{-3}. Previous molecular dynamics calculations of thermodynamic quantities for water have been carried out using an array processor by Rapaport and Scheraga[65,102] who studied a sample of 343 rigid waters using the CI potential with long runs and by Swope, Andersen, Berens, and Wilson[73] who studied the properties of water clusters. The software used previously[99,100] has been augmented by an intermolecular force and energy calculator for water as implemented by Swope and Andersen.[103] This calculator utilizes a piecewise fifth order polynomial fitted to the analytical potential energy functions as a function of the square of the distance between the two atoms being considered. It thus both allows a general algorithm to evaluate the polynomial previously fitted to arbitrary analytic functions and eliminates the necessity of a square root operation.

The method for applying a switching function as developed by Andersen and Swope smooths each water–water energy contribution to zero as the corresponding oxygen–oxygen distance passes through the switching region, which for our system extended from 0.85 to 0.90 nm. This technique eliminates the problem of artificially created monopoles (and possibly large dipoles) normally encountered by an atom–atom force feathering or truncation method as only part of the water passes through the feathering region (and is possibly imaged). This artifact is especially pronounced with water unless the Andersen–Swope technique is used as the partial charges on each atom are relatively large.

The semiempirical flexible water molecule potential developed by Watts[97] is used. The intermolecular potential is pairwise by atoms and fitted to the second virial coefficient of steam. The intramolecular potential is a standard Taylor's series in internal coordinates about the potential minimum as derived from vibrational spectroscopy.[98]

Equilibration of the initial water system is accomplished by following periods of dynamics (0.1–2.0 ps)

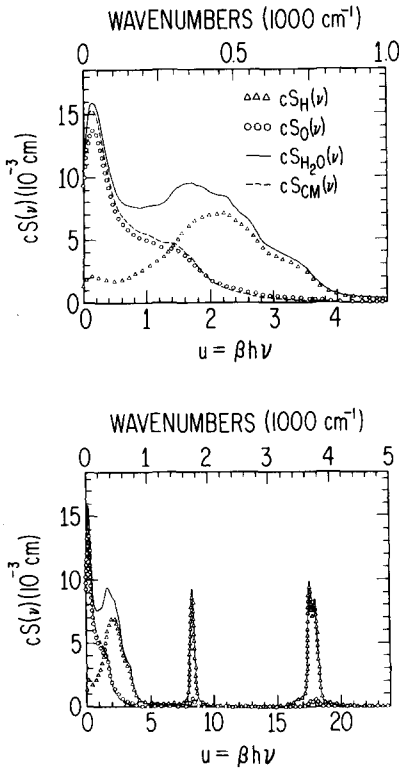

FIG. 2. Velocity spectra times the speed of light c normalized for one molecule of H_2O at 300 K and 1.0 g cm^{-3}, using the Watts potential with 250 waters and cubic periodic boundary conditions. The lower panel contains $cS_H(\nu)$ for the hydrogen atoms per molecule of water, $cS_O(\nu)$ for the oxygen atoms per molecule of water, the sum, $cS_H(\nu)+cS_O(\nu)=cS_{H_2O}(\nu)$, and the center-of-mass velocity spectrum $cS_{c.m.}(\nu)$. The upper panel is a blowup of the low frequency region of the lower panel. The lower horizontal scales are in terms of the reduced energy $u=\beta h\nu$. The speed of light c is included so that the integral of $cS(\nu)$ in cm vs the upper scale of wave numbers in cm^{-1} will be dimensionless, giving the total number of equivalent harmonic oscillators. For a purely harmonic system the velocity spectrum $S(\nu)$ would give the number of harmonic modes per unit frequency. Note that the H atoms dominate $S_{H_2O}(\nu)$ above 300 cm^{-1} and the O atoms below it.

with randomizations of velocity according to a Maxwell–Boltzmann distribution at the desired temperature until the temperature of the system stabilizes. The total simulation time involved in equilibration is approximately 60 ps. The time step of integration during equilibration is 0.5 fs while for the data collection a time step of 0.25 fs is used.

The velocity data is accumulated by selecting out the velocities every 12 time steps over a period of 50 000 time steps (12.3 ps total simulation time). A more elegant approach would be to use a digital low-pass filter before sampling.[104] The energy and heat capacity data are the result of a much longer series of seven runs for a total of 380 000 time steps over 95 ps.

C. Velocity spectra

The velocity spectra $S(\nu)$ shown in Fig. 2 are calculated by fast Fourier transforms of the velocity time histories of various components of the system. We define the following normalized velocity spectra

$$S_H(\nu) = \frac{4\pi\beta}{M}\sum_{j=1}^{2M} m_j^H \langle D[v_j^H(t)]\rangle \ , \tag{4.1}$$

$$S_O(\nu) = \frac{4\pi\beta}{M}\sum_{j=1}^{M} m_j^O \langle D[v_j^O(t)]\rangle \ , \tag{4.2}$$

$$S_{H_2O}(\nu) = S_O(\nu) + S_H(\nu) \ , \tag{4.3}$$

$$S_{CM}(\nu) = \frac{4\pi\beta}{M}\sum_{j=1}^{M} m_j^{H_2O} \langle D[v_j^{CM}(t)]\rangle \ , \tag{4.4}$$

where m^O, m^H, and m^{H_2O} represent the masses of an oxygen atom, hydrogen atom, and water molecule respectively; D is the spectral density operator defined in Eq. (3.2); $v_j^O(t)$, $v_j^H(t)$, and $v_j^{CM}(t)$ represent the velocity time histories of the jth oxygen atom, hydrogen atom and molecular center-of-mass, respectively; M is the number of water molecules, where $M \equiv N/3$; and a factor of $1/M$ has been introduced to normalize the velocity spectra to that for one molecule of water. The contribution to $S_{H_2O}(\nu)$ by both the oxygens and the hydrogens is determined by computing each spectrum $S_O(\nu)$ and $S_H(\nu)$ separately. The high frequency vibrational peaks composed mainly of the oxygen–hydrogen vibrations are easily seen in Fig. 2. The center-of-mass velocity spectrum of the system is also computed and its spectrum reflects the highly damped vibrational modes of whole water molecules.

The area under $S_{H_2O}(\nu)$ in Fig. 2 equals 9.0, the equivalent number of harmonic oscillators per molecule of water, as expected from Eq. (3.9). (The speed of light is introduced to make the integral vs cm^{-1} unitless.) The double peak in the range 2600–5000 cm^{-1}, which corresponds to the symmetric and asymmetric stretching modes of the water molecule, has an area of 1.89. The peak in the range 1200–2600 cm^{-1}, which corresponds to the bending of the HOH bond angle, has an area of 1.00. This substantiates the view of $S(\nu)$ as a density of normal modes and further suggests that the close association of the water molecules in the liquid phase has shifted some of the high frequency stretching motion down into the low frequency region.

In principle a potential with both intra- and intermolecular degrees of freedom like the WATTS potential we have used could take into account the frequency changes from gas to liquid. The actual frequencies for the WATTS potential for the gas phase should be close to the harmonic values[105] of $\nu_1 = 3832$ cm^{-1} (symmetric stretch), $\nu_2 = 1649$ cm^{-1} (bend), $\nu_3 = 3943$ cm^{-1} (asymmetric stretch), compared to the computed liquid phase peaks centered at 3680, 1740, and 3760 cm^{-1} as shown in Fig. 2. In real water, the infrared and Raman spectra show the gas phase anharmonic frequencies[106] to be 3652, 1595, and 3756 cm^{-1} and the liquid phase[9,107] shows a bending peak at approximately 1650 cm^{-1} and a broad stretching peak centered at approximately 3400 cm^{-1} with perhaps a subsidiary peak at approximately 3200 cm^{-1}. Thus the WATTS vibrational shifts from gas to liquid phase qualitatively resemble the real water shifts with large shifts downward in frequency for the stretching motions and a smaller shift upward for the bending motion, but the agreement is certainly not quantitative.

From $S_{CM}(0)$ in Fig. 2 and Eq. (3.16) we obtain for the center-of-mass diffusion coefficient $\bar{D}$ of water a value of 4.08×10^{-9} $m^2\,s^{-1}$ compared to the experimental value[108,109] of 2.42×10^{-9} $m^2\,s^{-1}$ for liquid water at 300 K. The precision of our reported value is questionable because we selected out every twelfth velocity rather than all velocities for the fast Fourier transform due to computer memory limitations, and a more reliable value could be computed from the asymptotic slope of the mean square displacement of the center-of-mass for a long molecular dynamics run. It should also be remembered that the finite size of the periodic boundaries may affect the longest wavelength and lowest frequency motions and in particular that hydrodynamic or concerted motions involving many molecules may not be accurately handled.

Berendsen *et al.*[55] have reported a spectral density of the center-of-mass of rigid molecule liquid water, using the SPC potential, which is strikingly similar to our $S_{CM}(\nu)$. They report a diffusion coefficient of 3.6×10^{-9} $m^2\,s^{-1}$.

D. Quantum corrections

The difference between the classical and quantum mechanical weighting functions $W(\nu)$ arises from the difference between the classical and quantum harmonic oscillator partition functions $q(\nu)$. In the classical limit of $h \to 0$, or equivalently $u \to 0$, $\nu \to 0$, or $T \to \infty$, this distinction disappears,

$$\lim_{h\to 0} q^Q(\nu) = \lim_{h\to 0} q^C(\nu) \ . \tag{4.5}$$

This implies

$$\lim_{h\to 0} W^Q(\nu) = \lim_{\nu\to 0} W^Q(\nu) = \lim_{\nu\to 0} W^C(\nu) \tag{4.6}$$

and thus,

$$W^\Delta(0) = W^Q(0) - W^C(0) = 0 \tag{4.7}$$

in all cases, as can be seen in Fig. 1. The divergence of $W^Q(\nu)$ from $W^C(\nu)$ as ν increases results in a preferential weighting of high frequency motions in the calculation of quantum corrections.

Table I gives the liquid water quantum corrections computed from the velocity spectrum $S_{H_2O}(\nu)$ from Eqs. (4.1)–(4.3) as shown in Fig. 2 and the quantum correction weighting functions $W^\Delta(\nu)$ as shown in Fig. 1, using Eqs. (3.45)–(3.48). The curves of the products of $S(\nu)$ and W^Δ for the energy, heat capacity, free energy, and entropy are shown in Figs. 3–6, illustrating the contribution to the quantum corrections as a function of frequency and of atom type. A separation is made for the purposes of Table I in frequency space at 1200 cm^{-1} between the intermolecular and intramolecular motions for liquid water. Note that the intermolecular motions, the hindered translation, and rotation, contribute substantially to the total quantum corrections.

Classically, a harmonic oscillator contributes k_BT to the energy regardless of frequency as a result of equipartition of energy. This produces a straight line for the classical weighting function in the top panel of Fig. 1. Quantum mechanics, however, requires that a

TABLE I. Inter- and intramolecular contributions to liquid water quantum corrections at 300 K per mole.

	Inter (0–1200 cm^{-1})	Intra (1200–5000 cm^{-1})	Total
E^{Δ} (kJ)	4.2	45.0	49.2
C_v^{Δ}(J/K)	−11.0	−23.8	−34.8
A^{Δ} (kJ)	2.2	33.4	35.6
S^{Δ} (J/K)	6.5	38.8	45.3

harmonic oscillator contain a minimum or zero point energy of $h\nu/2$. For a harmonic oscillator with $h\nu \ll k_B T$, this requirement is unimportant and quantum effects are small. In contrast, a harmonic oscillator with $h\nu \gg k_B T$ has an average energy near $h\nu/2$. As a result

$$\lim_{\nu\to\infty} W_E^Q(\nu) = u/2 = \beta(h\nu/2) . \tag{4.8}$$

Thus the quantum effects are large for a high frequency harmonic oscillator as it contributes $h\nu/2$ to the energy instead of $k_B T$. Table I shows a value of 49.2 kJ for the total quantum correction to energy. Others have accounted for this quantum effect by introducing a constant into the potential energy function. Using spectroscopic data, Eisenberg and Kauzmann[9] have calculated 55.45 kJ as a zero point energy.

Heat capacity is unique in that it results in a negative quantum correction, and it has the most significant contribution from the low frequency region compared to the other corrections we have listed. As a result of equipartition of energy, the classical harmonic oscillator contributes k_B to C_v regardless of frequency. This produces a straight line in the next to the top panel of Fig. 1. In contrast, the quantum mechanical harmonic oscillator with $h\nu \gg k_B T$ is "stuck" in the ground state and changes very little in response to changes in temperature. As a result,

$$\lim_{\nu\to\infty} W_{C_v}^Q(\nu) = 0 . \tag{4.9}$$

Thus, for each harmonic oscillator with $h\nu \gg k_B T$, k_B must be subtracted from the classically calculated C_v. The importance of the low frequency contribution to the quantum correction for constant volume heat capacity results from the rapid divergence of $W_{C_v}^Q(\nu)$ and $W_{C_v}^C(\nu)$ as ν increases from zero.

The equation $A = E - TS$ holds in an analogous manner for the quantum corrections as a result of the linear form of the quantum correction equations. The energy term dominates for harmonic oscillators and thus the quantum correction for free energy is always positive.

The reader may be surprised that the quantum correction for entropy is positive. A quantum mechanical har-

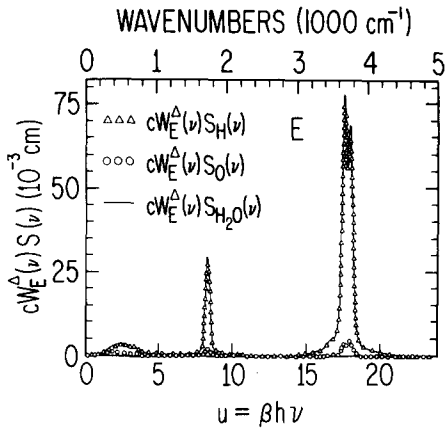

FIG. 3. Energy quantum correction curves for liquid water for H atoms, for O atoms, and their sum giving the total H_2O. Plotted is the product of the speed of light c, the velocity spectrum $S(\nu)$, and the energy quantum correction weighting function $W_E^{\Delta}(\nu)$ vs the reduced oscillator $u \equiv \beta h\nu$ on the bottom axis and the wave number equivalent at 300 K on the top axis. The integral of the product $S(\nu)\,W_E^{\Delta}(\nu)$ vs ν gives the quantum correction to energy, as shown in Eq. (3.45). The figure also illustrates how the quantum correction partitions between the O atoms and the H atoms which dominate at all but the lowest frequencies.

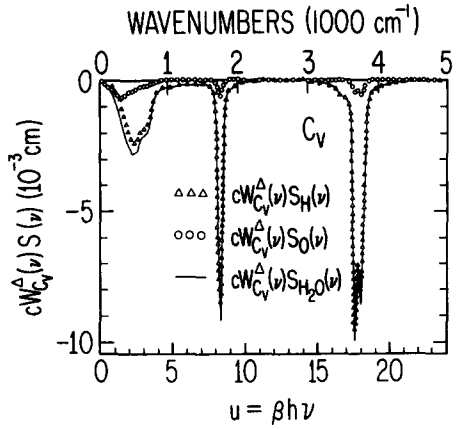

FIG. 4. Constant volume heat capacity quantum correction curves for liquid water for H atoms, for O atoms, and their sum giving the total H_2O quantum correction. The integral of the product $S(\nu)\,W_{C_v}^{\Delta}(\nu)$ vs ν gives the quantum correction to constant volume heat capacity, as shown in Eq. (3.46).

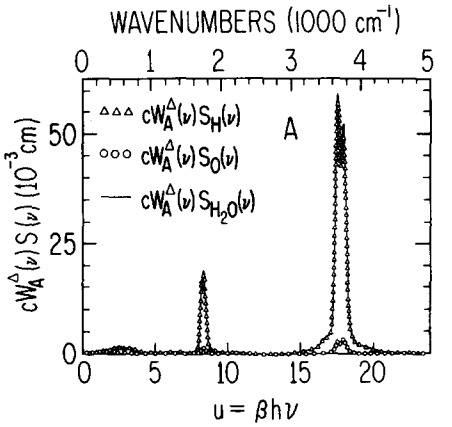

FIG. 5. Helmholtz free energy quantum correction curves for liquid water for H atoms, for O atoms, and their sum giving the total H_2O quantum correction. The integral of the product $S(\nu)\,W_A^{\Delta}(\nu)$ vs ν gives the quantum correction to Helmholtz free energy, as shown in Eq. (3.47).

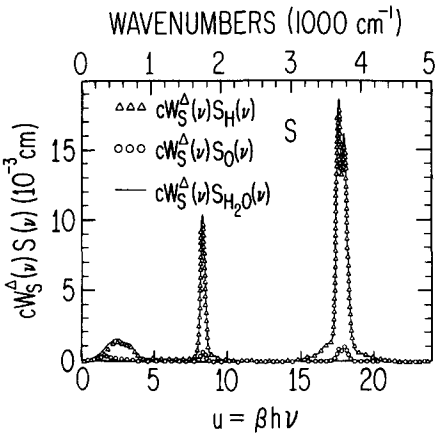

FIG. 6. Entropy quantum correction curves for liquid water for H atoms, for O atoms, and their sum giving the total H_2O quantum correction. The integral of the product $S(\nu)\,W_S^\Delta(\nu)$ vs ν gives the quantum correction to entropy, as shown in Eq. (3.48).

monic oscillator with $h\nu \gg k_B T$ is stuck in the ground state and contributes almost nothing to the entropy. Thus, as seen in Fig. 1,

$$\lim_{\nu \to 0} W_S^Q(\nu) = 0 \,. \tag{4.10}$$

In contrast, the classical harmonic oscillator weighting function has the following properties:

$$\lim_{\nu \to 0} W_S^C(\nu) = \infty \,, \tag{4.11}$$

$$\lim_{\nu \to \infty} W_S^C(\nu) = -\infty \,. \tag{4.12}$$

The first equation indicates that an unconstrained particle has an unlimited number of available states. The second equation results from the difficulty of applying the third law of thermodynamics to the classical representation of entropy for a harmonic oscillator. Because of the negative sign of the classical weighting function, the quantum correction for entropy is positive.

Figures 3–6 show the products of the velocity spectra $S(\nu)$ with the quantum correction weighting functions $W^\Delta(\nu)$ for energy E, constant volume heat capacity C_v, Helmholtz free energy A, and entropy S. Since $S_{H_2O}(\nu)$ can be partitioned into separate contributions from the hydrogen and oxygen atoms, we also partition the products $S_{H_2O}(\nu)W^\Delta(\nu)$ and thus compute separately the hydrogen and oxygen atom contributions to the quantum corrections. The hydrogen atom motions dominate except at the very lowest frequencies which have little weight anyway.

E. Energy

Seven water samples with different energies are created and equilibrated, and the average temperature for each sample, calculated over at least 10 ps running time, is plotted in Fig. 7. A straight line is fitted to the points, and the total classical energy E^C corresponding to 300 K is calculated. By averaging over a subset (500 time steps selected over a time period of 1.25 ps) of a complete run at 300 K we also compute the average value of the intramolecular potential energy V_{intra}; the intermolecular potential energy V_{inter}; and the kinetic energy E_k as shown in Table II. Because E^C is calculated from the fitting shown in Fig. 7 while V_{intra}, V_{inter}, and E_k are calculated from the short subset discussed above, there is a 0.1 kJ mol^{-1} discrepancy between the values shown in Table II for E^C and for the sum of its components $V_{\text{intra}} + V_{\text{inter}} + E_k$. The quantum correction E^Δ is obtained by integrating the function $S(\nu)\,W_E^\Delta(\nu)$ as shown in Eq. (3.45) and Fig. 3. Addition of the kinetic energy (calculated from instantaneous velocities[73,110]) to the total potential energy results in conservation of energy to one part in 30 000 with the 0.25 fs integration step size used. As suggested by Andersen[111] we graphed the standard deviation of the total energy vs the time step squared for several molecular dynamics runs. The resulting linear plot verified the accuracy of our computer package as the Verlet integration[110,112] algorithm gives an error in total energy in proportion to the square of the integration time step used. To calculate V_{intra}, we first remove a constant representing the zero point energy contribution from the original WATTS intramolecular potential.[97]

TABLE II. Energy (kJ mol^{-1}).

V_{intra}	5.2
V_{inter}	−42.1
E_k	11.2
E^C	−25.6[a]
E^Δ	49.2
$E^{\text{theor}} = E^C + E^\Delta$	23.6
E^{exptl}	21.5[b]

[a]Calculated from Fig. 7.
[b]See Table IV.

McDonald and Klein[75] calculate an intermolecular potential energy of −33 kJ mol^{-1} for the WATTS potential for 273 K and 1 g cm^{-1} and Reimers and Watts[57] report an intermolecular potential energy of −36.6 kJ mol^{-1} for the WATTS potential at 298 K and 0.997 g cm^{-1}. Both

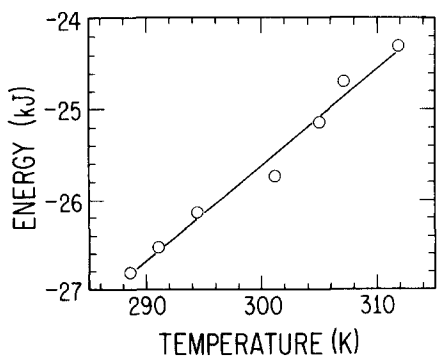

FIG. 7. Calculation of the classical energy E as well as the classical constant volume heat capacity C_v by least squares linear fit of E with respect to T. Values of the average temperature T are calculated from the kinetic energy E_k for microcanonical molecular dynamics run of at least 10 ps at each of seven different energies.

TABLE III. Energies in kJ mol^{-1} with standard deviations given in parentheses, bond lengths, and bond angle distortions for several cutoff and featuring boundary methods.

Type	V_{intra}	V_{inter}	E^c	$\frac{\overline{\delta r}}{r_{eq}}$ (%)	$\frac{\overline{\delta \vartheta}}{\vartheta_{eq}}$ (%)
ANDERSEN	5.2 (0.22)	−42.1 (0.26)	−25.8 (0.000 99)	0.52	−1.0
CUTOFF I	5.5 (0.32)	−58.8 (6.1)	−41.8 (6.4)	0.56	−1.0
CUTOFF II	5.5 (0.32)	−50.4 (0.45)	−33.6 (0.029)	0.56	−1.0
AA SMOOTH	27.5	−111.7		1.8	−1.7
IG	4.7			0.2	−0.1

calculations above differ from the present one in that their water molecules are constrained to be rigid. To determine the effect of this we increased the force constants on our waters by a factor of first 4 and then 16 while decreasing the time step first by 2 and then by 4. The result is that the intermolecular potential energy decreases (becomes more negative) with changes on the order of 1 to 2 kJ, indicating that the introduction of flexible waters increases (makes less negative) the intermolecular potential energy over a rigid water calculation. Reimers and Watts run at 298 K and the 1 atm density of 0.997 g cm^{-1} compared to our temperature and 85 atm density of 300 K and 1.0 g cm^{-1}. We performed a special test run at 0.977 g cm^{-1} and 298 K and calculated an intermolecular potential energy only marginally different from the first value, in line with the 0.012 kJ mol^{-1} shift expected[101] from experimental thermodynamic measurements. We perform a molecule-by-molecule imaging with force feathering technique following Andersen[103] rather than molecule-by-molecule potential cut-offs as used by Reimers and Watts or Ewald sums as used by McDonald and Klein. To explore the effects of potential or force smoothing or cutoff, we performed several additional test runs whose results are summarized in Table III. The standard deviations are given within parentheses and a time step of 0.25 fs is used for each run.

Perhaps the best way to compare[111] flexible water molecular dynamic and rigid water Monte Carlo calculations is to compare the difference in energy of the liquid and vapor states. For the Monte Carlo runs by Reimers *et al.*[57] this value is merely the intermolecular potential energy, −36.61 kJ mol^{-1}. For a flexible molecule calculation the heat of vaporization is the intermolecular potential energy for the liquid plus the difference in intramolecular potential energy upon the phase transition from liquid to gas. For our system $\Delta E = -42.1 + 5.2 - 4.7 = -41.6$ kJ mol^{-1}. The experimental value[94] is −41.0 kJ mol^{-1} at 300 K, and −41.4 kJ mol^{-1} at 298 K.

Boundary effects are a significant problem for systems like liquid water where the long range Coulombic forces extend well beyond the dimensions of the model. One way to deal with these nonzero forces near the boundary is to choose a cutoff distance beyond which the potential energy is set to zero. For an atom–atom central force system, this cutoff of the potential can be carried out atom by atom (CUTOFF I in Table III), and the resulting forces necessary for molecular dynamics calculations are then the derivatives of the potential within the cutoff distance and zero beyond, with a delta function at the boundary which being of measure zero in length is never seen by the dynamics calculation. Such energy-force pairs are inconsistent due to the effective neglect of the delta function force term at the cutoff distance and which prevents conservation of energy in actual molecular dynamics runs as required for microcanonical systems as the atoms failing to feel the force delta function can drift back and forth over the cutoff boundary with resulting large potential energy fluctuations. For ordinary Monte Carlo systems where forces are not needed, this difficulty is avoided. We suspect however that the large fluctuations in the radial distribution function, which occur at the cutoff distance, introduce significant perturbations to the system. Table III shows the results of a sample molecular dynamics calculation using a cutoff of 0.875 nm at the midpoint of the 0.85 to 0.90 nm Andersen–Swope feathering which we used for our actual thermodynamic calculations. Notice that the standard deviation (in parenthesis) for the intermolecular potential energy is a full 57% of the kinetic energy.

By cutting off the potential molecule-by-molecule using either the distance between the two centers-of-mass or the very similar oxygen–oxygen distance (as Andersen has done in his molecule-by-molecule smoothing method) as the functional variable, the effectively neglected delta function force terms used in molecular dynamics calculations are reduced significantly in magnitude as they now represent truncated dipole–dipole rather than monopole–monopole interactions. Molecule-by-molecule cutoff is also preferable to atom-by-atom cutoff for Monte Carlo calculations as the fluctuations in the radial distribution function at the cutoff distance should be greatly reduced.

One way to conserve energy in molecular dynamics runs while still using the atom-by-atom cutoff method is to set the atom–atom potential beyond the cutoff distance to its value at the cutoff distance (CUTOFF II). The energy-force pair is now consistent and for molecules like water where the forces are essentially Coulombic at the cutoff distance (and the total charge on each molecule is zero) the energy contribution for a molecule–molecule interaction conveniently sums to zero when all the atom–atom interactions are beyond the cutoff distance. The results for this method are

also shown in Table III. Note the order of magnitude reduction in the standard deviation of the total energy. In both cutoff methods, waters have a tendency to "straddle" the cutoff distance boundary in such a way as to reduce repulsive and increase attractive atom–atom interactions. For CUTOFF II, this has a negligible effect as the potential energy for any atom–atom interaction changes little across the boundary. For CUTOFF I, however, each atom–atom potential energy function is truncated to zero at the cutoff distance which causes an artificially low intermolecular potential energy, an effect in this case of 8.2 kJ mol^{-1}.

Another method which might seem reasonable in order to create a consistent energy-force system for molecular dynamics calculations is to smooth each atom–atom potential separately to zero (AA SMOOTH) in some smoothing region and then take the derivative to obtain the force. Indeed such a technique might be useful for systems where the value of the potential at the cutoff distance is near zero. For water this is not the case, however, and AA SMOOTH is totally useless in this application. For our test run we smoothed each potential to zero from 0.85 to 0.90 nm, and the corresponding force was calculated. The resulting energy values as shown in Table III differ drastically from experimental ones mainly due to the large fluctuations in the radial distributions near the cutoff distance. Large forces (20–30 times larger than for the unsmoothed potential) in the smoothing region cause such fluctuations and are a result of the steep slope of the potential necessary to smooth it to zero. One might view this effect as similar to smoothing the neglected delta function force term of the CUTOFF I system over 0.05 nm.

The technique by Andersen and Swope[103] (ANDERSEN) which smooths each entire water–water interaction to zero, thus eliminating the large forces of AA SMOOTH, may be viewed as smoothing the delta function force terms of molecule-by-molecule cutoff or equivalently dipole–dipole interactions over a small range, 0.05 nm in our case. It gives the best energy conservation and smallest V_{intra} and V_{inter} fluctuations as shown in Table III. In addition its waters are put under the least "stress" as measured by V_{intra}.

It may be concluded from the data in Table III that there are several advantages to using the ANDERSEN method. It should also be noted that the choice of method of handling boundary effects significantly influences energy calculations with differences on the order of 10 kJ mol^{-1}.

Table III also contains information on the intramolecular energy, the bond lengths, and the bond angles for each system. V_{intra} may be seen as a rough index to the stress each water molecule is experiencing. For an ideal gas (IG), i.e., for the same intramolecular potential with the intermolecular potential turned off, the intramolecular energy at 300 K is 4.7 kJ mol^{-1}, 0.96 kJ mol^{-1} above the $3/2k_BT$ value of 3.74 kJ mol^{-1} one would expect if no anharmonic effects were found. In the liquid state, however, each oxygen–hydrogen bond on the average is stretched and each HOH angle on the average is reduced below the equilibrium value, thus increasing V_{intra} above the ideal gas level.

For a nonrigid calculation at 295.4 K using the LS potential, Rahman, Stillinger, and Lemberg[69] report $V_{\text{intra}} + V_{\text{inter}} = -34.8$ kJ mol^{-1}, while we calculate for WATTS at 300 K $V_{\text{intra}} + V_{\text{inter}} = -36.9$ kJ mol^{-1}. In their partitioning between V_{intra} and V_{inter} they assume, but do not measure, that V_{intra} is given by the expected undistorted harmonic oscillator values, an approximation which we see to be incorrect, at least in our case, due to anharmonicity and intermolecular force induced molecular distortion.

The experimental value to which the calculated intermolecular energies should be compared deserves some discussion as two significantly different numbers are quoted throughout the literature. One way to obtain the intermolecular potential energy of liquid water is to equate it to the difference in energy of the fluid and vapor states. This is calculated by subtracting PV from the heat of vaporization of water at 300 K. Using this method, Dashevsky and Sarkisov[94] obtain for the intermolecular potential energy from experimental data -41.0 kJ mol^{-1} at 300 K, and -41.4 kJ mol^{-1} at 298 K. As pointed out by several workers,[36,56,57,113–116] however, the bending and stretching frequencies of water change upon condensation, and this difference in intramolecular energy must be accounted for, as well as the correction for conversion of free to hindered translation and rotation. Reimers *et al.*[57] calculate the resulting zero point energy shifts and estimate a correction on the order of 7.5 kJ mol^{-1} which would lead to an intermolecular potential energy of -33.9 kJ mol^{-1} for 298 K. Owicki and Scheraga[36] on the other hand use a slightly different method than Reimers *et al.*[57] and estimate a correction close to zero. As discussed in Sec. III, Owicki and Scheraga calculate the entire quantum intermolecular energy from spectra by making a harmonic approximation and subtract from that energy the classical potential energy to obtain their quantum correction. This may account for the variation in experimental intermolecular potential energy quoted in the literature, as some workers use the corrected value as calculated by Reimers *et al.*[57] some use the corrected value as calculated by Owicki and Scheraga,[36] while others use no correction at all.

The equivalent E^{expt} experimental value for total energy is the difference in energy between liquid water at 300 K and ideal noninteracting water vapor at 0 K with no zero point vibrational energy, measuring energies from the bottom of the potential well for noninteracting molecules. It may be calculated as follows:

$$E_{300\,\text{K}}(\text{liq}) - E_{0\,\text{K}}(\text{vap})$$
$$= [E_{300\,\text{K}}(\text{liq}) - E_{0\,\text{K}}(\text{ice})] + [E_{0\,\text{K}}(\text{ice}) - E_{0\,\text{K}}(\text{vap})] \quad (4.13)$$
$$\approx [H_{300\,\text{K}}(\text{liq}) - H_{0\,\text{K}}(\text{ice})] + [H_{0\,\text{K}}(\text{ice}) - H_{0\,\text{K}}(\text{vap})] \quad (4.14)$$

because $E \approx H$ for liquid water and ice. Including the zero point vibrational energy gives the results shown in Table IV.

Our computed $E^{\text{theor}} = 23.6$ kJ mol^{-1} and experimentally derived $E^{\text{expt}} = 21.5$ kJ mol^{-1} total energies as shown in Tables II and IV thus agree quite well, perhaps better

TABLE IV. Experimental total energy (kJ mol^{-1}).

$H_{300\,K}$(liq) $-H_{0\,K}$ (ice)	13.4[a]
$H_{0\,K}$ (ice) $-H_{0\,K}$(vap)	−47.36[b]
Vibrational zero point energy	55.45[b]
E^{expt}	21.5

[a]N. Dorsey, *Properties of Ordinary Water Substance* (Hafner, New York, 1968).
[b]D. Eisenberg and W. Kuazman, *The Structure and Properties of Water* (Oxford University, New York, 1969).

than expected in light of the possible improvements discussed in Sec. V below.

F. Heat capacity

The energy is fixed in a microcanonical ensemble while the temperature as computed from Eq. (2.6) fluctuates about an average value. Seven distinct water configurations with different energies are created, and the average temperature for each sample is calculated over at least 10 ps of running time. The seven points are plotted on the energy-temperature graph in Fig. 7. A straight line is fitted to the points, and the slope is calculated, giving the constant volume heat capacity. The results seen in Table V show quite good agreement with experiment once the quantum correction is added. Note that the calculated value would disagree substantially with experiment if the 11.0 J deg^{-1} mol^{-1} intermolecular quantum correction for hindered rotational and translational motion had been omitted.

V. DISCUSSION AND CONCLUSION

The calculations for liquid water presented here are designed to illustrate the quantum correction of classical thermodynamic quantities and not to provide the ultimate in accuracy for those thermodynamic values. Even though the results agree well with experiment, $E^{theor} = 23.6$ vs $E^{expt} = 21.5$ kJ mol^{-1}, and $C_v^{theor} = 71.7$ vs $C_v^{expt} = 74.5$ J deg^{-1} mol^{-1}, it is clear that these classical calculations could be improved. For example, it can be argued that no potential function yet exists for water which is adequate to represent both the inter- and intramolecular motions or which is even valid in an effective sense for all phases.[57,96] The WATTS potential function which we use in this example calculation is no exception, having been criticized[75] on the ground that radial distribution functions calculated from it do not agree with experiment. It is unlikely, as we've seen, to properly account for the change in vibrational frequencies[9,36,113–116] on going from the gas to the liquid phase, as there is no direct coupling between intermolecular distances and the intramolecular part of the potential. The reader is referred to the recent paper by Reimers, Watts, and Klein[57] for a comparison among various existing water potentials and a presentation of a revised WATTS potential. The potential we have used is clearly only an effective[34,117] molecule–molecule potential, as it omits three[34,60,61,77,80,118–121] (and higher) molecule effects which surely must exist. In addition, one could make a more accurate calculation by including a correction[6,15,36] for the tails of the potential beyond the 0.85–0.90 nm region at which we feathered the potential to zero or one could try other long range correction techniques such as Ewald sums.[122] It seems clear from the large variations in energy among different choices of boundary treatment that much more needs to be learned about the effects of different boundary treatments on systems with long range potentials and their convergence to experimental values. Related questions have been raised by Pangali, Rao, and Berne[90] with respect to Monte Carlo calculations. The methodology of quantum correction illustrated here would work equally well with any or all of the improvements mentioned above to the classical part of the calculations.

A substantial amount of calculation is needed to achieve the accuracy illustrated in Fig. 7. The long simulation time to achieve a stable average can be interpreted in terms of the unusual "stickiness" of liquid water.[82,89] The 95 ps of total molecular simulation time illustrated in Fig. 7 required 190 h of real time on an array processor.[99,100] The array processor speed is approximately 35 times[100] that achieved in optimized Fortran on a DEC VAX 11/780 with a floating point accelerator, and judging from previously reported figures,[89] 5–10 times faster than a rigid water calculation on an IBM 360/91. Our 2000 time steps/h when scaled for number of particles and cutoff radius is roughly comparable to the speed reported by Rapaport and Scheraga[65,102] for their array processor molecular dynamics calculation for rigid water, taking into account that they use a predictor–corrector integrator, while we only use one force evaluation per time step.

A very different way to compute dynamics and thermodynamic quantities which may in time become practical would be a quantum force classical trajectory approach[123] in which at each time step in the classical trajectory the forces (for the dynamics) and the energy (for the thermodynamics) are computed from *ab initio* quantum mechanics.

It is clear from these results that one can and should take into account quantum corrections in testing molecular potential functions against experimental thermodynamic measurements. In particular, the intermolecular (hindered translational and rotational) motions in strongly associated liquids can lead to signifi-

TABLE V. Constant volume heat capacity (J deg^{-1} mol^{-1}).

C_v^c	106.5
C_v^Δ	−34.8
$C_v^{theor} = C_v^c + C_v^\Delta$	71.7
C_v^{exptl}	74.5[a]

[a]D. Eisenberg and W. Kauzman, *The Structure and Properties of Water* (Oxford University, New York, 1969).

cant errors if the related quantum corrections are neglected in thermodynamic comparisons with experiment. Consider, e.g., that the intermolecular quantum correction to energy for our system is 38% of the kinetic energy while the intermolecular quantum correction to free energy is 20% of the kinetic energy. The intermolecular quantum correction to heat capacity is 15% of the experimental value while the intermolecular quantum correction for entropy is 10% of the experimental value.[101] Similarly, motions in polymers (which can themselves be affected by solvent interactions) may also need thermodynamic quantum correction, and the molecular dynamics method illustrated here also can be applied in such cases.

An interesting aspect of this quantum correction technique is that after the dynamics (which in general depend upon all the atoms) are computed, the quantum corrections may be calculated atom by atom, and thus the quantum effects on the thermodynamic variables may be considered separately for different elements, different chemical environments of the same element, different types of molecules, or molecules in different environments. An advantage of the basically classical molecular dynamics approach to thermodynamics presented here is the ability to visualize and understand intuitively the classical motions and frequencies responsible for thermodynamic effects. For example, one can understand in a very pictorial way the dominance of the water quantum corrections by the hydrogen atom motions as illustrated in Figs. 3–6.

This technique for quantum correcting classical thermodynamic quantities should be applicable to a wide variety of molecular systems including polymers such as proteins and nucleic acids, liquids, solutions, and solids. For example, the molecular dynamics method could be used to compute and quantum correct the heat capacity of biomolecules in solution, a quantity known to depend on molecular conformation. Thermodynamic calculations can be made involving both intermolecular and intramolecular degrees of freedom. In addition, this approach can be extended to treat quasiequilibrium cases, such as the calculation of thermodynamic quantities as a function of progress along a chemical reaction coordinate or thermodynamic quantities for molecules in special surroundings such as boundary waters near a protein.

ACKNOWLEDGMENTS

We thank William C. Swope and Hans C. Andersen for many helpful discussions and the use of their array processor water intermolecular force calculation software and the Office of Naval Research, Chemistry, the National Science Foundation, Chemistry, and the National Institutes of Health, both General Medical Sciences and Division of Research Resources, for providing the support which has made this work possible.

[1]D. A. McQuarrie, *Statistical Mechanics* (Harper and Row, New York, 1976).
[2]H. C. Andersen, J. Chem. Phys. **72**, 2384 (1980).
[3]J. L. Lebowitz, J. K. Percus, and L. Verlet, Phys. Rev. **153**, 153 (1967).
[4]P. S. Y. Cheung, Mol. Phys. **33**, 519 (1977).
[5]J. G. Kirkwood, J. Chem. Phys. **3**, 300 (1935).
[6]J. A. Barker and D. Henderson, Rev. Mod. Phys. **48**, 587 (1976).
[7]M. Mezei, S. Swaminathan, and D. L. Beveridge, J. Am. Chem. Soc. **100**, 3255 (1978).
[8]R. J. Harrison, J. A. Cox, G. H. Bishop, and S. Yip, in *Computer Simulation for Materials Application*, edited by R. J. Arsenault, J. R. Beeles, and J. A. Simmons (NBS Nuclear Metallurgy, Washington, D.C., 1976), Vol. 20, p. 604.
[9]D. Eisenberg and W. Kauzmann, *The Structure and Properties of Water* (Oxford University, New York, 1969).
[10]E. Wigner, Phys. Rev. **40**, 749 (1932).
[11]J. G. Kirkwood, Phys. Rev. **44**, 31 (1933).
[12]J. G. Kirkwood, J. Chem. Phys. **1**, 597 (1933).
[13]H. S. Green, J. Chem. Phys. **19**, 955 (1951).
[14]J.-P. Haneen and J.-J. Weis, Phys. Rev. **188**, 314 (1969).
[15]J. A. Barker, R. A. Fisher, and R. O. Watts, Mol. Phys. **21**, 657 (1971).
[16]E. J. Derderian and W. A. Steele, J. Chem. Phys. **55**, 5795 (1971).
[17]Y. Singh and J. Ram, Mol. Phys. **25**, 145 (1973).
[18]H. L. Lemberg and F. H. Stillinger, J. Chem. Phys. **62**, 1677 (1975).
[19]J. G. Powles and G. Rickayzen, Mol. Phys. **38**, 1875 (1979).
[20]E. D. Glandt, J. Chem. Phys. **74**, 1321 (1981).
[21]H. Fredrikze, Mol. Phys. **43**, 489 (1981).
[22]P. C. Hemmer, Phys. Lett. A **27**, 377 (1968).
[23]B. Jancovici, Phys. Rev. **178**, 295 (1969).
[24]B. Jancovici, Phys. Rev. **184**, 119 (1969).
[25]W. G. Gibson, Phys. Rev. A **5**, 862 (1972).
[26]W. G. Gibson, Mol. Phys. **30**, 1 (1975).
[27]W. G. Gibson, Mol. Phys. **30**, 13 (1975).
[28]B. P. Singh and S. K. Sinha, J. Chem. Phys. **67**, 3645 (1977).
[29]B. P. Singh and S. K. Sinha, J. Chem. Phys. **68**, 562 (1978).
[30]B. P. Singh and S. K. Sinha, J. Chem. Phys. **69**, 2927 (1978).
[31]B. P. Singh and S. K. Sinha, J. Chem. Phys. **70**, 552 (1979).
[32]J. D. Doll and L. E. Myers, J. Chem. Phys. **71**, 2880 (1979).
[33]R. P. Feynman and A. R. Hibbs, *Quantum Mechanics and Path Integrals* (McGraw–Hill, New York, 1965).
[34]F. Stillinger, Adv. Chem. Phys. **31**, 1 (1975).
[35]G. E. Uhlenbeck and L. Gropper, Phys. Rev. **41**, 79 (1932).
[36]J. C. Owicki and H. A. Scheraga, J. Am. Chem. Soc. **99**, 7403 (1977).
[37]P. H. Berens and K. R. Wilson, J. Chem. Phys. **74**, 4872 (1981).
[38]P. H. Berens, S. R. White, and K. R. Wilson, J. Chem. Phys. **75**, 515 (1981).
[39]E. O. Brigham, *The Fast Fourier Transform* (Prentice–Hall, Englewood Cliffs, 1974).
[40]W. Marshal and S. W. Lovesey, *Theory of Thermal Neutron Scattering* (Oxford University, London, 1971).
[41]K. R. Symon, *Mechanics* (Addison–Wesley, Reading, Mass., 1964).
[42]F. G. Stremler, *Introduction to Communication Systems* (Addison–Wesley, Reading, Mass., 1977).
[43]P. Barnes, in *Progress in Liquid Physics*, edited by C. A. Croxton (Wiley, Chichester, 1978), p. 391.
[44]D. W. Wood, in *Water, A Comprehensive Treatise, Recent Advances*, edited by F. Franks (Plenum, New York, 1979), Vol. 6, p. 279.
[45]D. L. Beveridge, M. Mezei, P. K. Mehrotra, R. T. Marchese, G. R.-S. T. Vasu, and S. Swaminathan, in *Molecular-Based Study and Prediction of Fluid Properties*, Adv. Chem. Ser., edited by J. M. Haile and G. A. Mansoori (American Chemical Society, Washington, D.C., 1983).
[46]S. P. Goel and R. W. Hockney, Rev. Bras. Fis. **4**, 121 (1974).

[47]J. D. Bernal and R. H. Fowler, J. Chem. Phys. **1**, 515 (1933).
[48]J. S. Rowlinson, Trans. Faraday Soc. **47**, 120 (1951).
[49]A. Ben-Naim and F. H. Stillinger, in *Structure and Transport Processes in Water and Aqueous Solutions*, edited by R. A. Horne (Wiley–Interscience, New York, 1972).
[50]F. H. Stillinger and A. Rahman, J. Chem. Phys. 60, 1545 (1974).
[51]L. L. Shipman and H. A. Scheraga, J. Phys. Chem. **78**, 909 (1974).
[52]F. Stillinger and A. Rahman, J. Chem. Phys. **68**, 666 (1978).
[53]R. A. Nemenoff, J. Snir, and H. A. Scheraga, J. Phys. Chem. **82**, 2527 (1978).
[54]F. T. Marchese, P. K. Mehrotra, and D. L. Beveridge, J. Phys. Chem. **85**, 1 (1981).
[55]H. J. C. Berendsen, J. P. M. Postma, W. F. van Gunsteren, and J. Hermans, Jerusalem Symp. Quantum Chem. Biochem. **14**, 331 (1981).
[56]W. L. Jorgensen, J. Chem. Phys. **77**, 4156 (1982).
[57]J. R. Reimers, R. O. Watts, and M. L. Klein, Chem. Phys. **64**, 95 (1982).
[58]H. Popkie, H. Kistenmacher, and E. Clementi, J. Chem. Phys. **59**, 1325 (1973).
[59]O. Matsuoka, M. Yoshimine, and E. Clementi, J. Chem. Phys. **64**, 1351 (1976).
[60]F. H. Stillinger and C. W. David, J. Chem. Phys. **69**, 1473 (1978).
[61]J. M. Goodfellow, J. L. Finney, and P. Barnes, Proc. R. Soc. London Ser. B **214**, 213 (1982).
[62]F. H. Stillinger and A. Rahman, J. Chem. Phys. **57**, 1281 (1972).
[63]F. H. Stillinger and A. Rahman, in *Molecular Motions in Liquids*, edited by J. Lascombe (Reidel, Dordrecht, Holland, 1974), pp. 478–494.
[64]A. Geiger, A. Rahman, and F. H. Stillinger, J. Chem. Phys. **70**, 263 (1979).
[65]D. C. Rapaport and H. A. Scheraga, Chem. Phys. Lett. **78**, 491 (1981).
[66]A. Rahman and F. H. Stillinger, J. Chem. Phys. **55**, 3336 (1971).
[67]F. H. Stillinger and A. Rahman, J. Chem. Phys. **61**, 4973 (1974).
[68]A. Rahman and F. H. Stillinger, Phys. Rev. A **10**, 368 (1974).
[69]A. Rahman, F. H. Stillinger, and H. L. Lemberg, J. Chem. Phys. **63**, 5223 (1975).
[70]W. F. van Gunsteren, H. J. C. Berendsen, and J. A. C. Rullmann, Faraday Discuss. Chem. Soc. **66**, 58 (1978).
[71]M. Mezei, Chem. Phys. Lett. **74**, 105 (1980).
[72]R. W. Impey, M. L. Klein, and I. R. McDonald, J. Chem. Phys. **74**, 647 (1981).
[73]W. C. Swope, H. C. Andersen, P. H. Berens, and K. R. Wilson, J. Chem. Phys. **76**, 637 (1982).
[74]I. McDonald and M. Klein, Faraday Discuss. Chem. Soc. **66**, 48 (1978).
[75]I. R. McDonald and M. Klein, J. Chem. Phys. 68, 4875 (1978).
[76]R. O. Watts, Mol. Phys. **32**, 659 (1976).
[77]P. Barnes, J. L. Finney, J. D. Nicholas, and J. E. Quinn, Nature (London) **282**, 459 (1979).
[78]E. Clementi, *Determination of Liquid Water Structure. Coordination Numbers for Ions and Solvation for Biological Molecules* (Springer, Berlin, 1976).
[79]S. Swaminathan and D. L. Beveridge, J. Am. Chem. Soc. **99**, 8392 (1977).
[80]J. M. Goodfellow, Proc. Natl. Acad. Sci. U.S.A. **79**, 4977 (1982).
[81]J. A. Barker and R. O. Watts, Mol. Phys. **26**, 789 (1973).
[82]M. Mezei, S. Swaminathan, and D. L. Beveridge, J. Chem. Phys. **71**, 3366 (1979).
[83]R. O. Watts, Mol. Phys. **28**, 1069 (1974).
[84]J. A. Barker and R. O. Watts, Chem. Phys. Lett. **3**, 144 (1969).
[85]H. Kistenmacher, H. Popkie, E. Clementi, and R. O. Watts, J. Chem. Phys. **60**, 4455 (1974).
[86]G. C. Lie and E. Clementi, J. Chem. Phys. **62**, 2195 (1975).
[87]G. C. Lie, E. Clementi, and M. Yoshimine, J. Chem. Phys. **64**, 2314 (1976).
[88]D. L. Beveridge, M. Mezei, S. Swaminathan, and S. W. Harrison, in *Computer Simulation of Bulk Matter from a Molecular Perspective*, edited by P. G. Lykos (American Chemical Society, Washington, D.C., 1978).
[89]M. Rao, C. Pangali, and B. J. Berne, Mol. Phys. **37**, 1773 (1979).
[90]C. Pangali, M. Rao, and B. J. Berne, Mol. Phys. **40**, 661 (1980).
[91]S. F. O'Shea and P. R. Tremaine, J. Chem. Phys. **84**, 3304 (1980).
[92]M. Mezei and D. L. Beveridge, J. Chem. Phys. 76, 593 (1982).
[93]G. N. Sarkisov, V. G. Dashevsky, and G. G. Malenkov, Mol. Phys. **27**, 1249 (1974).
[94]V. G. Dashevsky and G. N. Sarkisov, Mol. Phys. **27**, 1271 (1974).
[95]O. Weres and S. A. Rice, J. Am. Chem. Soc. **94**, 8983 (1972).
[96]M. D. Morse and S. A. Rice, J. Chem. Phys. **76**, 650 (1982).
[97]R. O. Watts, Chem. Phys. **26**, 367 (1977).
[98]K. Kuchitsu and Y. Morino, Bull. Chem. Soc. Jpn. **38**, 814 (1965).
[99]K. R. Wilson, in *Minicomputers and Large Scale Computations*, edited by P. Lykos (American Chemical Society, Washington, D.C., 1977), pp. 147–170.
[100]P. H. Berens and K. R. Wilson, J. Comp. Chem. (in press, 1983).
[101]N. Dorsey, *Properties of Ordinary Water Substance* (Hafner, New York, 1968).
[102]D. C. Rapaport and H. A. Scheraga, J. Chem. Phys. **86**, 873 (1982).
[103]T. Andrea, W. C. Swope, and H. C. Andersen, J. Chem. Phys. (submitted).
[104]R. K. Otnes and L. Enochson, *Applied Time Series Analysis, Basic Techniques* (Wiley–Interscience, New York, 1978).
[105]S. Califano, *Vibrational States* (Wiley, London, 1976).
[106]G. Herzberg, *Molecular Spectra and Molecular Structure. II. Infrared and Raman Spectra of Polyatomic Molecules* (Van Nostrand, Princeton, 1945).
[107]G. E. Walrafen, in *Water, A Comprehensive Treatise, The Physics and Chemistry of Water*, edited by F. Franks (Plenum, New York, 1972), Vol. 1, p. 151.
[108]R. Mills, J. Phys. Chem. **77**, 685 (1973).
[109]K. Krynicki, C. D. Green, and D. W. Sawyer, Faraday Discuss. Chem. Soc. **66**, 199 (1978).
[110]D. Beeman, J. Comput. Phys. **20**, 130 (1976).
[111]H. C. Andersen (private communication).
[112]L. Verlet, Phys. Rev. **159**, 98 (1967).
[113]M. G. Sceats, M. Stavola, and S. A. Rice, J. Chem. Phys. **70**, 3927 (1979).
[114]M. G. Sceats and S. A. Rice, J. Chem. Phys. **72**, 3236 (1980).
[115]M. G. Sceats and S. A. Rice, J. Chem. Phys. **72**, 3248 (1980).
[116]M. G. Sceats and S. A. Rice, J. Chem. Phys. **72**, 3260 (1980).
[117]F. Stillinger, J. Phys. Chem. **74**, 3677 (1970).
[118]H. Kistenmacher, G. C. Lie, H. Popkie, and E. Clementi, J. Chem. Phys. **61**, 546 (1974).
[119]E. Clementi, W. Kolos, G. C. Lie, and G. Ranghino, Int. J. Quantum Chem. **17**, 377 (1980).
[120]F. H. Stillinger, J. Chem. Phys. **71**, 1647 (1979).
[121]D. Hankins, J. W. Moskowitz, and F. H. Stillinger, J. Chem. Phys. **53**, 4544 (1970).
[122]J. P. Valleau and S. G. Whittington, in *Statistical Mechanics Part A: Equilibrium Techniques*, edited by B. J. Berne (Plenum, New York, 1977).
[123]D. R. Fredkin, A. Komornicki, S. R. White, and K. R. Wilson, J. Chem. Phys. **78**, 7077 (1983).